Analyst

RSC Publishing

PAPER

View Article Online
View Journal | View Issue

Label-free colorimetric sensing of copper(II) ions based on accelerating decomposition of H_2O_2 using gold nanorods as an indicator†

Cite this: *Analyst*, 2013, **138**, 2080

Shasha Wang,[ac] Zhaopeng Chen,*[a] Ling Chen,[ac] Ruili Liu[b] and Lingxin Chen*[a]

A novel label-free colorimetric strategy was reported for sensitive detection of copper ions (Cu^{2+}) by using the decelerating etching of gold nanorods (GNRs). H_2O_2 was employed as the oxidant for corrosion of GNRs, leading to the decrease of the aspect ratio of GNRs. In the absence of Cu^{2+}, the redox corrosion of GNRs by H_2O_2 occurred rapidly, causing the distinct color change of GNRs from bluish green to purplish red. By virtue of the strong and specific catalysis by Cu^{2+} of the decomposition of H_2O_2, the rate of redox corrosion can be decelerated. Relevant experimental parameters, including pH value, concentrations of NaSCN and H_2O_2, incubation temperature and time were evaluated. Under optimal conditions, our method gave a good linear range of 10–300 nM ($R = 0.9985$) for Cu^{2+} and the detection limit with the naked eye is as low as 10 nM. Thus, the proposed colorimetric sensor is simple, sensitive (4.96 nM) and selective, and it has been successfully applied to detect Cu^{2+} in shellfish samples. Moreover, the potential mechanism was also discussed.

Received 21st November 2012
Accepted 18th January 2013

DOI: 10.1039/c3an36722c

www.rsc.org/analyst

Introduction

Colorimetric detection methods are extremely attractive in chemical and biological analysis, as they require no sophisticated instrumentation and signal recognition can be achieved by the naked eye in the form of a color change. Compared with other detection methods, colorimetric detection also offers advantages of simplicity, rapidity, and cost-effectiveness. It is reported that a variety of signal reagents have been used in colorimetric assays, such as organic dyes,[1] polymers,[2] enzymes[3] and nanoparticles.[4] Among different kinds of signal reagents, gold nanorods (GNRs), which possess distinctive optical properties as a typical elongated metal nanostructure, have been proved to be of great use in colorimetric detections.[5] The UV-IR absorption spectrum of GNRs displays two peaks, one is the transverse surface plasmon resonance (TSPR) band and the other is the longitudinal surface plasmon resonance (LSPR) band. The LSPR band is so sensitive that a tiny change in surface binding environment will lead to an obvious wavelength shift.[6] Additionally, the extinction coefficient of GNRs ($\sim 10^9$ M^{-1} cm^{-1}) is larger than that of gold nanoparticles (2.7×10^8 M^{-1} cm^{-1}), and several orders of magnitude higher than those of traditional organic chromophores.[7] It is also important to mention that elongated nanomaterials are inherently more sensitive to the local dielectric environment, when compared to similar-sized spherical nanoparticles.[8] By virtue of the above advantages, GNRs have become a good candidate for sensor research.

The past few years have witnessed great progress in colorimetric detection based on GNRs.[9] One of the strategies is based on the aggregation of specific ligand modified GNRs. A variety of molecules (polymers, small molecules, DNA, *etc.*) can be joined to the surface of nanorods and the modifying molecules would be combined to different parts (end or side) of the surface due to the anisotropy of nanorods.[10] When a specific object is added, an obvious target induced aggregation of GNRs occurs by end-to-end linkages or side-by-side assembly *via* covalent bonding, hydrogen bonding or electrostatic interaction, along with the color change of colloid. For example, cysteine-modified GNRs were reported for the colorimetric detection of Cu^{2+}. In the presence of Cu^{2+}, the nanorods aggregated through longitudinal assembly due to the strong coordination between Cu^{2+} and cysteine (Cys–Cu–Cys), accompanied by a visible color change from blue-green to dark gray.[11] However, most aggregation based colorimetric strategies display some drawbacks, such as the complex synthetic procedures of crosslinkers and strong non-specific interactions. The other colorimetric strategy is based on the redox-regulated surface chemistry on GNRs. It is well known that the optical properties of GNRs are greatly affected by a small change in the shape and size.[12] Taking

[a]*Key Laboratory of Coastal Zone Environmental Processes and Ecological Remediation, Yantai Institute of Coastal Zone Research (YIC), Chinese Academy of Sciences (CAS), Shandong Provincial Key Laboratory of Coastal Zone Environmental Processes, YICCAS, Yantai 264003, China. E-mail: zhpchen@yic.ac.cn; lxchen@yic.ac.cn; Fax: +86-535 2109130; Tel: +86 535 2109133; +86-535 2109130*

[b]*School of Environment and Materials Engineering, Yantai University, Yantai 264005, China*

[c]*University of Chinese Academy of Sciences, Beijing 100049, China*

† Electronic supplementary information (ESI) available: Fig. S1–S5 and optimization of experimental conditions. See DOI: 10.1039/c3an36722c

advantage of this property, a variety of colorimetric methods have been presented involving wavelength changes in the absorption spectra of GNRs. For instance, in the presence of Br^- and Cl^- ions, the standard electron potential of Au(I)/Au(0) is lower than that of Cr(VI)/Cr(III), which enables GNRs to be oxidized by Cr(VI).[13] As a result, the redox etching caused an obvious decrease in length but only a slight change in diameter, presenting distinct color changes. A similar method was reported involving oxidation etching of GNRs induced by ferric chloride at room temperature.[14]

Recently, Fang *et al.* developed a colorimetric method for visual detection of Cu^{2+} based on the oxidative corrosion of gold nanoparticles.[15] In their presented method, H_2O_2 and SCN^- were employed as the oxidant and the ligand, respectively. Due to the catalysis by $Cu(NH_3)_6^{2+}$ of the decomposition of H_2O_2 in NH_3/NH_4Cl buffer, the oxidative corrosion of gold nanoparticles can be inhibited. The detection limit with the naked eye was down to 50 nM.

Inspired by this study, we designed a highly sensitive and selective colorimetric strategy based on the strong and specific inhibition of Cu^{2+} on the corrosion of GNRs in the absence of NH_3. Our proposed colorimetric method displays high sensitivity and selectivity and the detection limit by the naked eye is down to 10 nM. The sensing mechanism and practical application of the method in shellfish samples were also investigated and satisfactory results were obtained.

Experimental section

Chemicals

Cetyltrimethylammonium bromide (CTAB) and tris(hydroxymethyl) aminomethane (Tris) were purchased from Sigma. $CuSO_4 \cdot 5H_2O$ was obtained from Aladdin Industrial Incorporation. Hydrogen tetrachloroaurate(III) dehydrate ($HAuCl_4 \cdot 4H_2O$), sodium borohydride, sodium thiocyanate, hydrogen peroxide (~30%), ascorbic acid, HCl (36–38%), HNO_3 (65–68%) and other metal salts used were obtained from Sinopharm Group Chemical Reagent Co. Ltd (Beijing, China). All the reagents were of analytical grade and used without any further purification.

Apparatus

Solutions were prepared with deionized water (18.2 MΩ·cm specific resistance) purified by a Cascada LS Ultrapure water system (Pall Corp., USA). Transmission electron microscope (TEM) images were taken on a JEM-1230 electron microscope (JEOL Ltd, Japan) operating at 100 kV. UV-Vis absorption spectra were recorded on a Thermo Scientific NanoDrop 2000C spectrophotometer (Gene Company Ltd, USA).

Synthesis of GNRs

For preparation of GNRs a typical seed-mediated and CTAB surfactant-directed method was adopted with some necessary modification.[16] Briefly, 50 μL of 50 mM $HAuCl_4$ was added to 7.7 mL of 0.10 M CTAB solution upon stirring, and 0.30 mL of fresh, ice-cold 0.01 M $NaBH_4$ solution was put into the mixed solution, which resulted in the change of solution color from bright brown-yellow to pale brown. The obtained solution was stirred for another 2 minutes and kept at 28 °C as the seed solution for the next procedure. Then, 50 mL of 0.10 M CTAB solution was mixed with 600 μL of 50 mM $HAuCl_4$ with constant stirring. To this solution, 150 μL of 0.01 M $AgNO_3$ solution was added and 480 μL of 0.1 M ascorbic acid (AA) was added with gentle stirring, leading to the change of solution color from dark yellow to colorless. Subsequently, 100 μL of the seed solution was injected into the colorless solution at 28 °C. The mixture was stirred for another 20 minutes and the resultant colloid of GNRs was stored for future use.

Colorimetric assay process for Cu^{2+}

After optimization of the experimental conditions, the colorimetric detection of Cu^{2+} was tested under the selected conditions. The measurement was carried out in 50 mM Tris–HCl buffer solution (pH 8.7). 10 μL of 0.1 M NaSCN and 10 μL of 3 M H_2O_2 were subsequently dissolved in 800 μL of buffer solution containing 200 μL of the GNRs, and then 10 μL of different concentrations of Cu^{2+} were added to each of the mixture solutions. Finally, the mixture solutions were incubated in a 60 °C water bath for 17 minutes and the UV-Vis absorption spectra were recorded.

In the selectivity experiments, all samples were tested in a similar way. We investigated the selectivity of our approach for Cu^{2+} over other metal ions (Li^+, Na^+, K^+, Zn^{2+}, Al^{3+}, Mg^{2+}, Fe^{3+}, Mn^{2+}, Cd^{2+}, Pb^{2+}, Ni^{3+}, Cr^{3+}, Ag^+, As^{3+}, Hg^{2+}) under the same optimized conditions.

Analysis of real samples

Shellfish samples were digested with concentrated nitric acid.[17] Typically, by removing the outer shells, the obtained samples were washed with deionized water and then put into the refrigerator. Once frozen, the materials were placed in a freeze-dryer to remove water. After drying, the materials were ground to powder by mortars. To 0.3 g of powder sample, 10 mL concentrated nitric acid were added, and the mixtures were incubated in a high pressure digestion tank at 150 °C for 6 h. Finally, the obtained colorless solution was diluted to 50 mL.

To detect the concentration of Cu^{2+} in the real samples, a similar test to the above assay process was adopted, just using samples directly to replace copper solution.

Results and discussion

Sensing mechanism

The sensing mechanism for colorimetric detection of Cu^{2+} based on decelerating etching of GNRs is shown in Scheme 1. The UV-Vis absorption spectrum of the initial GNRs (length/diameter ratio about 2 : 1) exhibits two peaks located at 520 nm and 650 nm (Fig. 1(A), curve a), corresponding to the TSPR band and the LSPR band, respectively. When 1 mM NaSCN and 30 mM H_2O_2 were added to the colloidal solution, the LSPR band weakened and shifted to a shorter wavelength (Fig. 1(A), curve c) after incubation in a 60 °C water bath for 17 minutes with a color change from bluish green to purplish red. The

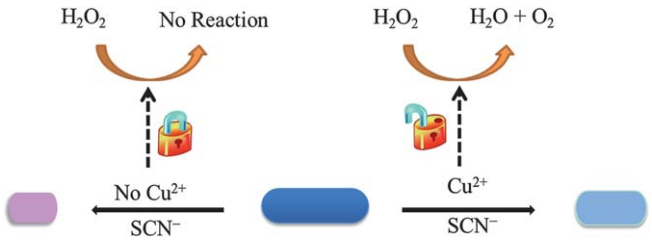

Scheme 1 Schematic mechanism for Cu^{2+} sensing based on decelerating etching of GNRs.

obvious color change resulted from the oxidation of GNRs by H_2O_2 in the presence of SCN^-. Because of the strength of the Au–S bond, SCN^- containing a thio-group can strongly coordinate with gold ions, replacing part of the CTAB on the surfaces of GNRs. The standard potential of $Au(SCN)_2^-/Au$ is 0.69 V in eqn (1), and the conditional potential of H_2O_2/H_2O is 1.24 V, calculated according to Nernst equation at pH 9.0 at room temperature. So gold can be easily oxidized by H_2O_2 and form $Au(SCN)_2^-$ complexes in solution. The total redox reaction can be described as $Au + 2SCN^- + H_2O_2 + 2H^+ \rightarrow Au(SCN)_2^- + 2H_2O$. On the contrary, the presence of 50 nM Cu^{2+} resulted in a slight blue shift of the LSPR band (Fig. 1(A), curve b) and the color of the solution was pale blue. According to the phenomenon we suggested that Cu^{2+} can catalyse the decomposition of H_2O_2 to inhibit the oxidative corrosion of GNRs. The differences among TEM images also indicated the inhibition of Cu^{2+} towards the etching of GNRs (Fig. 1(C)). The mechanism we put forward is different from Fang's *et al.*[15] In their report, it was $Cu(NH_3)_6^{2+}$ that could efficiently catalyse the decomposition of H_2O_2 in alkaline media to inhibit the etching of gold nanoparticles. In the absence of NH_3, the bare Cu^{2+} at low concentration had no significant inhibition.

$$Au(SCN)_2^- + e^- \rightarrow Au + 2SCN^- \quad E^{\ominus} = 0.69\ V \qquad (1)$$

$$H_2O_2 + 2H^+ + 2e^- \rightarrow 2H_2O \quad E^{\ominus} = 1.77\ V \qquad (2)$$

In order to further explore the potential mechanism of our proposed method, the residual H_2O_2 was finally estimated according to the intensity of the maximum absorption peak of potassium permanganate in 526 nm. As is shown in Fig. 1(B), when 10 μL of 3 M H_2O_2 was dissolved in 1 mL of buffer solution in the presence or absence of 1 mM NaSCN, the potassium permanganate was reacted completely (curve d and e), illustrating the catalytic decomposition of H_2O_2 did not occur. However, when 1 mM Cu^{2+} was added to the above two mixture solutions, the maximum absorption peaks of potassium permanganate in the absence of SCN^- (curve b) were a little higher than in the presence of SCN^- (curve c), showing the catalysis by Cu^{2+} of the decomposition of H_2O_2 was more remarkable in the presence of SCN^-. The major mechanism and the basic steps of the catalytic reaction have been shown on the basis of previous work.[18] Eqn (3) and (4) are fast and Cu^{2+} was reduced in the form of $[Cu^I(SCN)_n]^{1-n}$ and HO_2–Cu^I. Eqn (5)–(7) result in $OSCN^-$ autocatalysis, which is of great importance in

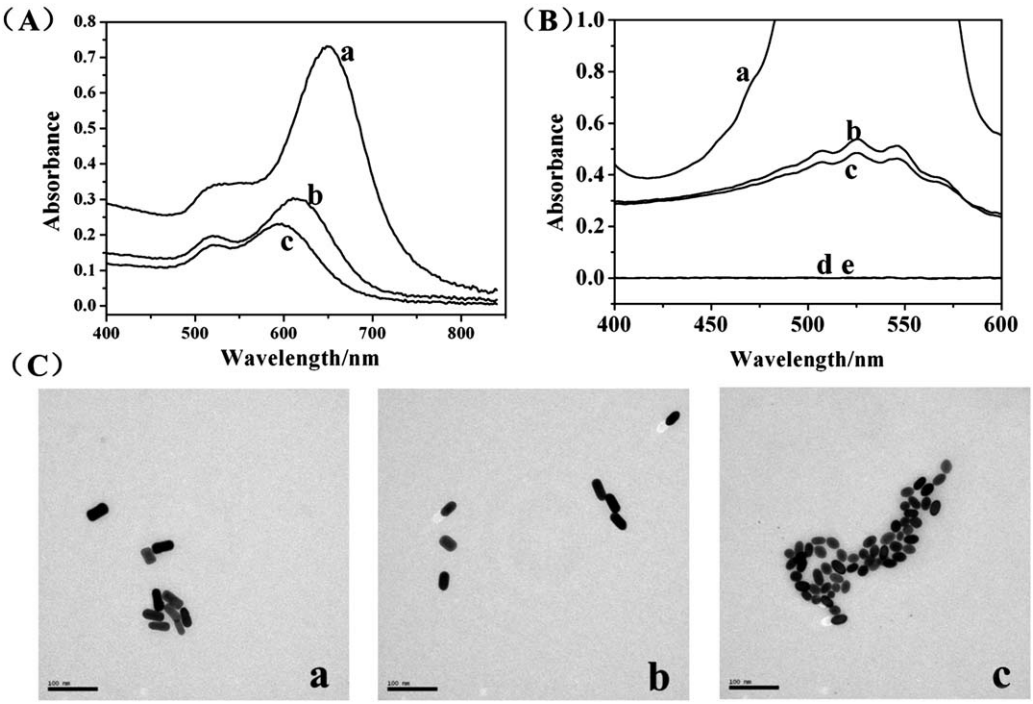

Fig. 1 (A) UV-Vis absorption spectra and (C) TEM images of before incubation (a) and after incubation in the presence (b) and absence (c) of 50 nM Cu^{2+} solution; (B) UV-Vis absorption spectra of potassium permanganate reacted with 1 mM NaSCN (a), 30 mM H_2O_2 + 1 mM NaSCN + 1 mM Cu^{2+} (b), 30 mM H_2O_2 + 1 mM Cu^{2+} (c), 30 mM H_2O_2 + 1 mM NaSCN (d), 30 mM H_2O_2 (e) after incubation, respectively.

the regeneration of SCN^- and $[Cu^{II}(SCN)_n]^{2-n}$ (eqn (8)). Among these reaction steps, the rate of oxidation of stable $[Cu^{I}(SCN)_n]^{1-n}$ was the rate-determining step of the reaction, deciding the main length of the catalytic reaction. Thus, H_2O_2 could be efficiently catalyzed in alkaline media in the absence of NH_3. What's more, SCN^- could not only reduce the oxidation reduction potential of GNRs, but also take part in the catalytic process of H_2O_2.

$$H_2O_2 + Cu^{2+} + OH^- \rightarrow HO_2\text{–}Cu^{I} + H_2O \quad (3)$$

$$HO_2\text{–}Cu^{I} + nSCN^- \rightarrow [Cu^{I}(SCN)_n]^{1-n} + HO_2^{\cdot} \quad (4)$$

$$H_2O_2 + SCN^- \rightarrow OSCN^- + H_2O \quad (5)$$

$$H_2O_2 + OSCN^- \rightarrow OOSCN^- + H_2O \quad (6)$$

$$OOSCN^- + SCN^- \rightarrow 2OSCN^- \quad (7)$$

$$[Cu^{I}(SCN)_n]^{1-n} + H_2O + OSCN^- \rightarrow [Cu^{II}(SCN)_n]^{2-n} + OH^{\cdot} + SCN^- + OH^- \quad (8)$$

Optimization of experimental conditions

For optimization of the colorimetric strategy, relevant experimental parameters, including pH value, concentrations of NaSCN and H_2O_2, incubation temperature and time were evaluated by the colloid color.

The influence of pH value on the performance of the GNRs colorimetric probe was carried out in a range from 7.5 to 8.9, obtained by adjusting the ratio of Tris to HCl. In the pH range 7.5–8.5, little oxidation of GNRs occurred because of the high rate of catalytic decomposition of H_2O_2, along with no obvious color change. With increasing pH value, the rate of catalytic reaction became slower, leading to the more extensive oxidation of GNRs (Fig. S1†). Thus, we chose 50 mM Tris–HCl buffer solution (pH 8.7) as the reaction media.

The effect of concentration of NaSCN was investigated over the range from 0.6 to 1.4 mM, as shown in Fig. S2.† With increasing concentration of NaSCN, the rate of the total redox reaction became faster. However, despite higher concentrations of NaSCN forming more stable complexes $[Cu^{I}(SCN^-)_n]^{1-n}$, the rate of oxidation of stable $[Cu^{I}(SCN^-)_n]^{1-n}$ became slower. Hence, we chose 1 mM NaSCN in the following studies.

The concentration of H_2O_2 was changed from 10 to 50 mM. The rate of catalytic reaction became faster with increasing concentration of H_2O_2. However, the redox corrosion of GNRs by H_2O_2 was also increased at the same time (Fig. S3†). In order to meet the needs of colorimetric detection, 30 mM H_2O_2 was chosen as a compromise.

Finally, the effect of incubation temperature and time was taken into consideration. As is observed in Fig. S4 and S5,† the etching of GNRs was dependent on both incubation temperature and time. The oxidative corrosion of GNRs increased with the increase of temperature at a fixed reaction time of 17 minutes. By setting the reaction temperature at 60 °C, the selective etching caused an obvious color difference in the absence and presence of 50 nM Cu^{2+} after reacting for 17 minutes. Thus, the reaction was performed by incubating the system for 17 minutes in the following studies.

Sensitivity and selectivity for Cu^{2+}

Fig. 2 shows the analytical performance of this method for the determination of Cu^{2+}. Under optimal detection conditions, a good linear relationship between the maximum absorbance of LSPR band and the concentrations of Cu^{2+} could be obtained in the range of 10 nM to 300 nM. The detection limit was 4.96 nM calculated by $3\sigma/S$.

To further realize the selectivity of our developed method, other metal ions, including Li^+, Na^+, K^+, Zn^{2+}, Al^{3+}, Mg^{2+}, Fe^{3+}, Mn^{2+}, Cd^{2+}, Pb^{2+}, Ni^{3+}, Cr^{3+}, Ag^+, As^{3+}, Hg^{2+} were examined under optimum conditions. As illustrated in Fig. 3, the presence of 100-fold Li^+, Na^+, K^+, Zn^{2+}, Al^{3+}, Mg^{2+}, Fe^{3+}, Mn^{2+}, 10-fold Cd^{2+}, Pb^{2+}, Ni^{3+}, $As^{3+}$and 1-fold Cr^{3+}, Ag^+, Hg^{2+} cannot catalysis the decomposition of H_2O_2 to inhibit the oxidative corrosion of GNRs; this can only occur with Cu^{2+}. In addition, the increase of Hg^{2+} concentration would affect the results because of the formation of $Hg(OH)_2 \rightarrow HgO$ capped on the rod, inhibiting the etching of gold. However, as a common metal ion in environmental samples, Cu^{2+} is normally present in greater concentrations than other ions, such as Cd^{2+}, Pb^{2+}, Ni^{3+}, As^{3+}, Cr^{3+}, Ag^+ and Hg^{2+}. As a consequence, the color of solution with Cu^{2+} was blue, while others are pale red. These results indicate the high selectivity of the proposed method.

Detection of Cu^{2+} in real samples

To evaluate the potential application of the proposed method, the detection of Cu^{2+} in shellfish samples was further carried out. As shown in Table 1, the recoveries ranged from 72.11% to 102.8%, which indicates the results obtained by this assay match well with those by ICP-MS, showing the high potential of the colorimetric method for Cu^{2+} quantification in real samples.

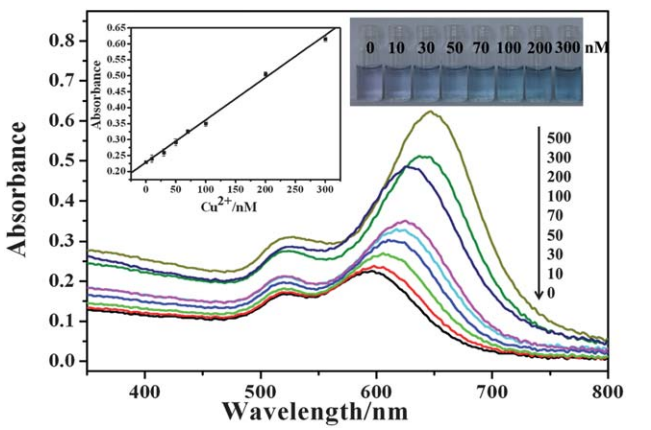

Fig. 2 UV-Vis absorption spectra of GNRs after incubation with different concentrations of Cu^{2+} for 17 minutes. Insets are a plot of the maximum absorbance of LSPR band *versus* the concentration of Cu^{2+} and the color changes with the increasing concentrations of Cu^{2+} from left to right, respectively.

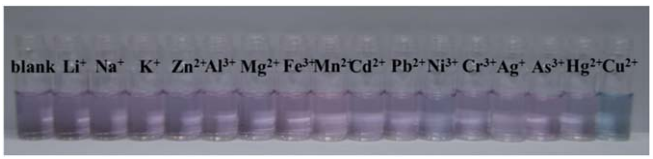

Fig. 3 Photo images of sensing GNRs solutions with 100 nM Cu^{2+}, Cr^{3+}, Ag^{+}, Hg^{2+}, 1 mM Cd^{2+}, Pb^{2+}, Ni^{3+}, As^{3+}, 10 mM Li^{+}, Na^{+}, K^{+}, Zn^{2+}, Al^{3+}, Mg^{2+}, Fe^{3+}, Mn^{2+}.

Table 1 Determination of Cu^{2+} in shellfish samples

Sample	Found by ICP-MS/ μM	Detected/μM	Recovery (%)
1	2.45	2.34	95.51
2	2.15	2.21	102.8
3	6.74	4.86	72.11

Conclusions

In conclusion, we have reported a highly sensitive and selective colorimetric method for the detection of Cu^{2+} based on GNRs. The present work takes advantage of catalysis by Cu^{2+} of the decomposition of H_2O_2 which could specifically inhibit the corrosion of GNRs, and we employ this system as the colorimetric probe. Additionally, our method shows sensitive and selective response towards Cu^{2+} ions without any other labelling or modification steps. Furthermore, the proposed approach exhibits great practicality for the detection of Cu^{2+} in real samples, which might present a promising potential for application in environmental monitoring.

Acknowledgements

This work was financially supported by the National Natural Science Foundation of China (grant no. 21275158), the Innovation Projects of the Chinese Academy of Sciences (grant no. KZCX2-EW-206), the Department of Science and Technology of Shandong Province (BS2009DX006), the Scientific Research Foundation for the Returned Overseas Chinese Scholars, State Education Ministry, and the 100 Talents Program of the Chinese Academy of Sciences.

Notes and references

1 (*a*) N. T. Greene and K. D. Shimizu, *J. Am. Chem. Soc.*, 2005, **127**, 5695–5700; (*b*) V. Vichai and K. Kirtikara, *Nat. Protoc.*, 2006, **1**, 1112–1116; (*c*) E. Palomares, M. V. Martinez-Diaz, T. Torres and E. Coronado, *Adv. Funct. Mater.*, 2006, **16**, 1166–1170; (*d*) C. Yu, J. Zhang, R. Wang and L. Chen, *Org. Biomol. Chem.*, 2010, **8**, 5277–5279.

2 (*a*) H. A. Ho, M. Boissinot, M. G. Bergeron, G. Corbeil, K. Dore, D. Boudreau and M. Leclerc, *Angew. Chem., Int. Ed.*, 2002, **41**, 1548–1551; (*b*) C. Li, M. Numata, M. Takeuchi and S. Shinkai, *Angew. Chem., Int. Ed.*, 2005, **44**, 6371–6374; (*c*) A. Hennig, A. Hoffmann, H. Borcherding, T. Thiele, U. Schedler and U. Resch-Genger, *Anal. Chem.*, 2011, **83**, 4970–4974; (*d*) J. Isaad and F. Salauen, *Sens. Actuators, B*, 2011, **157**, 26–33.

3 (*a*) J. W. Liu and Y. Lu, *J. Am. Chem. Soc.*, 2003, **125**, 6642–6643; (*b*) Z. Wang, J. H. Lee and Y. Lu, *Adv. Mater.*, 2008, **20**, 3263–3267; (*c*) M. Liu, C. Jia, Q. Jin, X. Lou, S. Yao, J. Xiang and J. Zhao, *Talanta*, 2010, **81**, 1625–1629; (*d*) G. Song, C. Chen, J. Ren and X. Qu, *ACS Nano*, 2009, **3**, 1183–1189; (*e*) H. Wei, C. Chen, B. Han and E. Wang, *Anal. Chem.*, 2008, **80**, 7051–7055.

4 (*a*) S. Kim, J. Kim, N. H. Lee, H. H. Jang and M. S. Han, *Chem. Commun.*, 2011, **47**, 10299–10301; (*b*) X. Fu, L. Chen, J. Li, M. Lin, H. You and W. Wang, *Biosens. Bioelectron.*, 2012, **34**, 227–231; (*c*) Y. Chen, H. Chang, Y. Shiang, Y. Hung, C. Chiang and C. Huang, *Anal. Chem.*, 2009, **81**, 9433–9439; (*d*) L. Chen, T. Lou, C. Yu, Q. Kang and L. Chen, *Analyst*, 2011, **136**, 4770–4773; (*e*) T. Lou, L. Chen, Z. Chen, Y. Wang, L. Chen and J. Li, *ACS Appl. Mater. Interfaces*, 2011, **3**, 4215–4220.

5 (*a*) N. R. Jana, L. Gearheart and C. J. Murphy, *J. Phys. Chem. B*, 2001, **105**, 4065–4067; (*b*) Y. Y. Yu, S. S. Chang, C. L. Lee and C. R. C. Wang, *J. Phys. Chem. B*, 1997, **101**, 6661–6664.

6 P. K. Jain, X. H. Huang, I. H. El-Sayed and M. A. El-Sayed, *Acc. Chem. Res.*, 2008, **41**, 1578–1586.

7 M. A. El-Sayed, *Acc. Chem. Res.*, 2011, **34**, 257–264.

8 C. G. Wang and J. Irudayaraj, *Small*, 2008, **4**, 2204–2208.

9 (*a*) J. Wang, P. Zhang, C. M. Li, Y. F. Li and C. Z. Huang, *Biosens. Bioelectron.*, 2012, **34**, 197–201; (*b*) B. F. Pan, L. M. Ao, F. Gao, H. Y. Tian, R. He and D. X. Cui, *Nanotechnology*, 2005, **16**, 1776–1780; (*c*) G. Wang, Z. Chen and L. Chen, *Nanoscale*, 2011, **3**, 1756–1759.

10 (*a*) L. Wang, Y. Zhu, L. Xu, W. Chen, H. Kuang, L. Liu, A. Agarwal, C. Xu and N. A. Kotov, *Angew. Chem., Int. Ed.*, 2010, **49**, 5472–5475; (*b*) H. Huang, X. Liu, T. Hu and P. K. Chu, *Biosens. Bioelectron.*, 2010, **25**, 2078–2083; (*c*) C. V. Durgadas, V. N. Lakshmi, C. P. Sharma and K. Sreenivasan, *Sens. Actuators, B*, 2011, **156**, 791–797.

11 J. Liu, H. Wang and X. Yan, *Analyst*, 2011, **136**, 3904–3910.

12 N. R. Jana, L. Gearheart and C. J. Murphy, *J. Phys. Chem. B*, 2001, **105**, 4065–4067.

13 F. Li, J. Liu, X. Wang, L. Lin, W. Cai, X. Lin, Y. Zeng, Z. Li and S. Lin, *Sens. Actuators, B*, 2011, **155**, 817–822.

14 R. Zou, X. Guo, J. Yang, D. Li, F. Peng, L. Zhang, H. Wang and H. Yu, *CrystEngComm*, 2009, **11**, 2797–2803.

15 Y. Fang, J. Song, J. Chen, S. Li, L. Zhang, G. Chen and J. Sun, *J. Mater. Chem.*, 2011, **21**, 7898–7900.

16 B. Nikoobakht and M. A. El-Sayed, *Chem. Mater.*, 2003, **15**, 1957–1962.

17 D. Jures and M. Blanus, *Food Addit. Contam.*, 2003, **20**, 241–246.

18 (*a*) M. Orban, *J. Am. Chem. Soc.*, 1986, **108**, 6893–6898; (*b*) J. Amrehn, P. Resch and F. W. Schneider, *J. Phys. Chem.*, 1988, **92**, 3318–3320; (*c*) S. Sattar and I. R. Epstein, *J. Phys. Chem.*, 1990, **94**, 275–277; (*d*) Y. Luo, K. Kustin and I. R. Epstein, *J. Am. Chem. Soc.*, 1989, **111**, 4541–4548; (*e*) C. Zhao, J. Zheng, J. Xie, H. Liu and Q. Gao, *Luminescence*, 2011, **26**, 130–135.